Clim Dyn (2008) 31:615–631
DOI 10.1007/s00382-008-0390-x

U. Büntgen (&) D. Frank J. Esper
Swiss Federal Research Institute WSL, Dendro Sciences Unit,
8903 Birmensdorf, Switzerland
e-mail: buentgen@wsl.ch

H. Grudd
Department of Physical Geography and Quaternary Geology,
Stockholm University, 10691 Stockholm, Sweden

temperature amplitude of the past millennium (Esper et al. 2005b). On the global-scale, we know of only ten (5) MXD-based chronologies that reflect summer temperatures back to AD 1200 (1000), of which three extend forward into the twenty-first century (Fig. 1c). A large-scale network compilation of MXD chronologies remains absent.

Increasing data paucity back in time is also a general rule at the regional-scale including the European sector (hereinafter EU), for which the pioneering work by Lamb (1965) is still referenced for the occurrence of relatively warm EU conditions during medieval times, the so-called Medieval Warm Period (MWP). Hence, the annually-resolved comparison of the EU 2003 summer heat (Luterbacher et al. 2004; Schär et al. 2004) with earlier warm periods still lacks confidence (Büntgen et al. 2006b). Nevertheless, significant progress has recently been made in understanding EU climate variability over the past 150 to about 500 years through studies of long instrumental station records (Auer et al. 2007 and references therein), documentary evidences (Brázdil et al. 2005 and references therein), tree-ring chronologies (Büntgen et al. 2007a; Frank and Esper 2005b), and multi-proxy compilations (Luterbacher et al. 2004), for example. Detailed knowledge of atmospheric circulation patterns over recent centuries is reported for the Alps (Casty et al. 2005), and the North Atlantic/EU sector (Luterbacher et al. 2002; Raible et al. 2006 and references therein). Reconstructions of synoptic-scale precipitation variability are developed using grid-box data (Pauling et al. 2006), and more locally using tree-ring chronologies (Esper et al. 2007; Wilson et al. 2005). In southern EU, temperature sensitive proxies with tree-rings in particular become sparse as such archives predominantly depend upon constrained thermal boundaries. For a detailed review of Mediterranean climate variability and change over the last centuries and the availability of existing proxies, the reader is referred to Luterbacher et al. (2006). Dendroclimatological studies from the Central Pyrenees are limited to TRW data from living trees (e.g., Camarero et al. 1998; Gutiérrez 1991; Rolland and Schueller 1994; Ruiz-Flaño 1988; Tardif et al. 2003). Existing studies mainly focus on the estimation of high to mid frequency variations, as missing relict material hinders the preservation of lower frequency variations via age-related composite tree-ring detrending methods (Briffa et al. 1992; Esper et al. 2003). Lower resolution archives, such as chrysophyte cysts from lake sediments collected at 1200 lakes from higher elevations in the Central and Eastern Pyrenees, revealed long-term information of winter/spring

Fig. 1 a *Regional-scale*: Location of the newly developed GER and SOB chronologies in the Spanish Pyrenees. *Black star* indicates the location of the high-elevation Pic du Midi instrumental station. b *European-scale*: Location of the summer temperature reconstructions from the Pyrenees (PYR), Alps (VAL) and Scandinavia (TOR). c *Hemispheric-scale*: Location of currently available MXD chronologies likely suitable to reconstruct variations in summer temperatures back to at least AD 1200 (CAM, Szeicz and MacDonald 1995; TOR, Grudd 2008; POL, Briffa et al. 1995; JAM, Briffa et al. 1995; QUE, Wang et al. 2001; GOT, Esper et al. 2002; ICE, Luckman and Wilson 2005; LAU, Schweingruber et al. 1988; VAL, Büntgen et al. 2006b), and this study (PYR). The TOR, VAL and PYR chronologies all extend into the twenty-first century

temperature fluctuations in the northwestern Mediterranean region (Pla and Catalan 2005).

With respect to the past millennium and EU, only a few temperature sensitive composite TRW records (i.e., combining recent and relict wood) exist from northern Scandinavia (Briffa et al. 2007; Helama et al. 2005) and the Alps (Büntgen et al. 2005; Nicolussi and Patzelt 2000), but none from the Mediterranean region. In addition, many of the existing tree-ring sites were sampled in the 1970–1980s, and thus miss the most recent warming trend seen in instrumental station measurements across the greater Alpine region (Auer et al. 2007).

Here we present the first tree-ring dataset combining samples of living and dry-dead timberline wood from the Central Spanish Pyrenees that reaches back prior to AD 1000 and extends forward into the twenty-first century (924–2005). As this study was performed to best preserve inter-annual to multi-centennial scale summer temperature variations, MXD measurements were processed for a selection of 261 cores that meet distribution criteria necessary for an optimized estimation of long-term trends. Age-related tree-ring detrending and variance adjustment methods were applied for chronology development, and various meteorological datasets considered for the analysis of monthly resolved growth/climate responses, calibration exercises, and spatial field correlations. Results allowed the full range of regional high to low frequency May-September maximum temperatures to be estimated for the past eight centuries. This southern EU temperature history was first compared with latest findings from the Alps and Scandinavia and then with prominent large-scale reconstructions, all covering the past millennium.

2 Data and methods

2.1 Tree-ring data and detrending

Two timberline sites: Gerber and Sobrestivo (hereinafter GER and SOB) of nearly similar ecological and climatic conditions were considered for the sampling of living and dry-dead (preserved on dry ground) pine (*Pinus uncinata* Ram.) trees of all age-classes. The GER site (42°41′N, 1°06′E) is located at the northern limit of the d'Aigüestortes I Estany de Sant Maurici National Park. The SOB site (42°41′N, 0°06′E), ≈ 70 km west of the GER site, is situated between the Ordesa y Monte Perdido National Park and the French border (Fig. 1a). *Pinus uncinata* Ram. is a shade-intolerant species dominating the sub-alpine vegetation belt in the Central Pyrenees between 1,600 and 2,500 m asl (e.g., Tardif et al. 2003). In elevations of 2,200–2,450 m asl, living trees and in situ relict samples were collected in open forests with wide talus slopes (Fig. 2). MXD measurements were performed for a selection of 261 tree-ring series with evenly distributed start and end dates through time (Fig. 3). Inter-series correlation (the average correlation coefficient amongst all pairs of series) of this dataset is 0.50, calculated after individual series detrending using cubic smoothing splines with a 50% frequency-response cutoff of equal to 32 years and over 50-year windows shifted by 25 years. The individual segment length (i.e., the number of rings per sample) ranges from 11 to 732 years. Mean segment length is 214 years. Means of 208 and 235 years are obtained for the GER and SOB subsamples, respectively. The average MXD is 0.64 g/cm^3, with little difference between the GER (0.63 g/cm^3) and SOB (0.66 g/cm^3) material. Average growth rate of 0.81 mm varies little between the GER (0.82 mm) and SOB (0.75 mm) sites.

To remove non-climatic, age-related growth trends from the raw TRW and MXD measurement series (Fritts 1976), while allowing lower frequency information above the mean segment length to be preserved (Cook et al. 1995), the regional curve standardization method (RCS; Briffa et al. 1992; Esper et al. 2003) was applied *via* ARSTAN (Cook 1985). Series were first aligned by cambial age (considering pith-offset estimations), a mean of these age-aligned series calculated, and this mean smoothed using a cubic spline of 10% the series length (Cook and Peters 1981). The resulting smoothed time-series is termed a regional curve (RC) and used for detrending, i.e., deviations of the individual measurement series from the RC were calculated as ratios. Dimensionless indices were then dated back to calendar years, and averaged using the arithmetic mean to form a chronology. The variance in the mean chronology was stabilized using methods introduced by Osborn et al. (1997), and those improved by Frank et al. (2007b). These include a time dependent '100-year moving window' approach for adjusting temporal changes in both, sample replication and inter-series correlation. Ninety-five percent of bootstrapped confidence limits were considered to estimate uncertainty in the mean value function (Efron 1987). To test for potential population and/or ecological differences between the GER (203 series) and SOB (58 series) data, and to evaluate the low frequency information captured by the RCS method, two site chronologies covering the AD 924–2005 and 1499–2005 periods were computed (Fig. 4). Signal strength of the final RCS chronologies was assessed using a 30-year 'moving window' approach of the inter-series correlation (*Rbar*), and the expressed population signal (*EPS*; Wigley et al. 1984). Cubic smoothing splines as described by Cook and Peters (1981) were used for time-series filtering.

Novel MXD-based reconstructions from the Swiss Alps (Valais; Büntgen et al. 2006b) and northern Sweden (Torneträsk; Grudd 2008) allowed a millennial-long

Fig. 2 The two timberline sites Gerber (*GER*) and Sobrestivos (*SOB*) within the Central Spanish Pyrenees, characterized by wide talus slopes and open pine forests

comparison of European-wide summer temperatures for the first time to be robustly performed (Fig. 1b) (Table 1). The Alpine June–September temperature reconstruction (AD 755–2004) contains 180 larch (*Larix decidua* Mill.) measurement series from living trees and historic construction timbers (Büntgen et al. 2006c). This record explains * 55% of summer temperature variations in the greater Alpine region and appears to capture the full range of past temperature variability, i.e., the well-known extreme years 1816 and 2003, warmth during medieval and recent times, and cold in between. It indicates positive temperatures in the tenth and thirteenth century that resemble twentieth century conditions, and displays a prolonged cooling from * 1350 to 1700. Six of the ten warmest decades over the full 755–2004 period are recorded in the twentieth century (for details see Büntgen et al. 2006b). The Scandinavian April–August temperature reconstruction (AD 501–2004) represents a major update of the original version that ended in 1980 (Briffa et al. 1992; Schweingruber et al. 1988). Measurements from 35 new pine (*Pinus sylvestris* L.) series now reach until 2004. This new Torneträsk reconstruction explains * 65% of regional summer temperature variability and captures the most recent warming trend. This revised history tells higher temperatures during medieval times in comparison to those published by Briffa et al. (1992) and Grudd et al. (2002) using MXD and TRW, respectively. Four periods of warmer summers than those obtained for the twentieth century fall 750, 1000, during the fifteenth century and * 1750 (for details see Grudd 2008).

2.2 Meteorological data and statistical analysis

Monthly minimum and maximum temperatures from the Pic du Midi mountain observatory (Pic du Midi de Bigorre: 2,862 m asl, 43°04′N, 0°09′E) that start in 1882 were used for proxy calibration. While the temperature data are described to have sufficient quality (Böhner and Dessens

Fig. 3 a Temporal distribution of the 203 GER (*red*) and b 58 SOB (*blue*) core samples ordered by calendar age of their innermost ring. Note the reduction in sample size <5 series prior to AD 1260. Black dots show sample distribution if series were ordered by their outermost ring. c Mean cambial age of the GER and SOB samples for each calendar year. d Regional curves (*RCs*) of the age-aligned GER and SOB MXD (*left*) and TRW (*right*) series (truncated <20 series at the series outermost end)

1991; Dessens and Bücher 1995), less value is reported for the precipitation measurements (Dessens and Bücher 1997). A 5 × 5 grid of homogenized and variance adjusted land and sea surface temperature data back to 1850 was used for spatial field correlations (HadCRUT3v; Brohan et al. 2006). For comparison with the Pic du Midi station measurements and the MXD-based estimates, we selected values from a single grid-box centered over 42.5 N and 2.5 E. The HadCRUT3v grid was considered as temperatures of the 1850–2003 period and their homogenization allows longer-term trends to be reasonably well preserved (Brohan et al. 2006). Since precipitation sums were, however, not available from this compilation, monthly temperature means and precipitation sums from a higher resolution (0.5 × 0.5) grid were utilized for twentieth century (1901–2002) growth/climate response analyses (CRUTS2.1; Mitchell and Jones 2005). Mean values from 42 grid-boxes covering the 42–43 N and 2 W–3 E region, and averages from three longitudinal sub-regions (0–2 W, 0–2 E, 2–3 E) were selected. Due to the shorter period covered, the interpolation techniques performed, and the homogenization applied, potential longer-term trends in this data are not fully preserved (see details in Mitchell and Jones 2005).

To estimate local-scale climatic conditions, particularly those of the GER site, three nearby high-elevation instrumental station records were kindly provided by the Meteorological Institute of Catalonia: *BONAIGUA* (2,263 m asl, 42 40 N, 1 06 E), *SANT MAURICI* (1,920 m asl, 42 34 N, 1 00 E), and *ESTANY-GENTO* (2,120 m asl, 42 30 N, 1 00 E). Mean annual temperature (1961–1990) of the three stations is 4.3 C (2.1 SD). Lowest (−2.5 C; 2.5 SD) and highest (13.1 C; 1.3 SD) monthly values are reported for January and July, respectively. Mean annual temperature averaged over four 30-year reference windows (1931–1960, 1941–1970, 1951–1980 and 1971–2000) ranges from 3.3 to 4.6 C (1.9–2.2 SD). Mean annual precipitation averaged over these periods ranges from 1,170 to 1,300 mm (± 58 to 65 SD). The evenly distributed amount of annual precipitation most likely results from the high-elevation location of the instrumental stations (and study sites), which are receiving a constant flow of

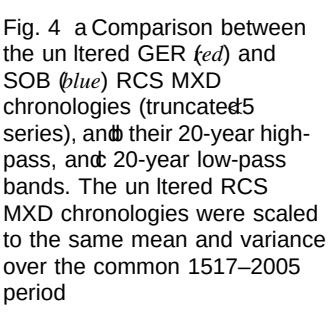

Fig. 4 a Comparison between the unfiltered GER (*red*) and SOB (*blue*) RCS MXD chronologies (truncated ≥5 series), and b their 20-year high-pass, and c 20-year low-pass bands. The unfiltered RCS MXD chronologies were scaled to the same mean and variance over the common 1517–2005 period

Table 1 Characteristics of the three MXD datasets used to reconstruct long-term regional-scale summer temperature variations

Record	Country	Lat/long	Elevation	Species	Series	AGR	Period	Record	Lag-1	Season
Scandinavia	Sweden	68°N/19°E	340	PISY	100	0.58	441–2004	501–2004	0.37	AMJJAS
Alps	Switzerland	46°N/08°E	2,000	LADE	180	0.87	735–2004	755–2004	0.64	JJAS
Pyrenees	Spain	42°N/01°E	2,400	PIUN	263	0.64	924–2005	1260–2005	0.14	MJJAS

Elevation = m asl, AGR = g/cm^3, Period = full length, Record = reconstructed period, Lag-1 = autocorrelation at 1 year, Season = reconstructed seasonality

maritime (Atlantic) air masses all year long. Data were transformed to anomalies with respect to 1961–1990, and significance levels 'conservatively' corrected for *lag-1* autocorrelation (Trenberth 1984).

A split calibration/verification approach was performed to assess temporal stability of the transfer model, with the following metrics being considered: Pearson's correlation coefficient (r), reduction of error (RE), and Coefficient of Efficiency (CE). Both RE and CE are measures of shared variance between actual and estimated series (CE is a more rigorous verification statistic), with a positive value suggesting that the reconstruction has some skill (Cook et al. 1994).

3 Results and discussion

3.1 Chronology characteristics

Regional curves and RCS chronologies were separately calculated for TRW and MXD data of the GER and SOB sites. While estimated TRW growth trends are remarkably similar at both sites (Fig. 3d), a slight but systematic level offset between the MXD growth trends is seen. The RC based on the 58 SOB series indicates generally higher density compared to the RC of the 203 GER series, with largest differences found during juvenile growth. Resulting RCS chronologies of the GER and SOB MXD measurements correlate at 0.53 over their common 1517–2005 period of ≥5 series (Fig. 4a), with little differences (0.57 and 0.49) being obtained from their 20-year high- and low-pass fractions (Fig. 4b, c).

To account for the differing MXD growth rates between GER and SOB, two independent RCs were used for RCS detrending on a site-by-site level. The detrended 203 GER and 58 SOB index series were then averaged to create the final, variance adjusted Pyrenees chronology (hereinafter PYR). To avoid potential biases during the record's period of site overlap, we shifted the 58 SOB series by the average difference between the GER and SOB mean records over 1517–2005. This systematic offset is minimal with a mean difference of 0.0013 index units.

EPS values of the PYR chronology meet signal strength acceptance from ~ 1300 to present (Fig. 5a), referring to robust mean-value functions (Wigley et al. 1984). Figure 5b, c compares the new PYR time-series with and without variance adjustment. Variance of the uncorrected record slightly increases back in time. While sample replication constantly decreases before ~ 1700, *Rbar* values tend to increase back in time, and thus likely account for most of the trend in the variance behavior of the uncorrected PYR chronology. After variance adjustment, the PYR chronology is characterized by mitigated changes in variability (Fig. 5c), with the variance increase prior to ~ 1730 diminished. Running standard deviation measurements of the chronologies after consideration of differing variance adjustment methods show the removal of relative variance in ation due to changes in both sample replication and inter-series correlation (Fig. 5d). Even though methods described by Osborn et al. (1997) already result in a clear variance reduction, additional improvement due to the technique introduced by Frank et al. (2007b) helps further stabilizing the time-series. The variance adjustments applied to the nal PYR chronology yield to a less biased estimate of local summer temperature variability, as local variance depends less on changes in sample structure and replication. *Lag-1* autocorrelation of this record is 0.14 over the AD 1260–2005 time-span, re ecting little biological memory (i.e., persistence of previous year growth conditions) in the MXD parameter. Note that *lag-1* autocorrelation of the maximum, minimum and mean May–September temperature data is 0.23, 0.56, and 0.28, respectively (1882–2005).

Fig. 5 a *EPS* and *Rbar* statistics (calculated over 30 years lagged by 15 years) of b the PYR chronology (AD 1260–2005) without variance adjustment, and replication. The *horizontal dashed line* in a denotes the 0.85 *EPS* criterion for signal strength acceptance (Wigley et al. 1984). *Grey shading* in b denotes 95% bootstrap con dence levels of the smoothed RCS chronology. c The nal PYR chronology after variance adjustment, and d moving 31-year standard deviations of the chronologies without variance adjustment (*blue*), using variance adjustment for changes in sample replication (*black*), and variance adjustment for changes in sample replication and *Rbar* (*red*). Smoothed curves in b and c are 20-year low-pass lters

3.2 Growth/climate responses

Correlation analysis between the MXD-based PYR chronology and climate data from individual station records and various subgroups of gridded data was undertaken over maximum periods of overlap (Fig. 6). Signi cant ($p < 0.01$) correlation to March and August, and various seasonal temperature means of the current year are revealed. The May–September seasonal average of maximum temperatures (1901–2002) derived from the Pic du Midi station yields highest correlation with PYR ($r = 0.52$). Correlations between PYR and current year June and July temperatures, along with those of the previous year and all precipitation sums are found to be non-signi cant. For a better understanding of the growth/climate response in the MXD parameter, similar correlations were computed for TRW and a combination of both parameters (Fig. 6). Correlations between TRW and maximum temperatures are found to be non-signi cant (with the exception of previous year October). Correlations between TRW and mean/minimum temperatures reveal signi cant ($p < 0.01$) response to previous year October, current year May and the May–August and May–September means. A similar response pattern is gained from the MXD/TRW hybrid. Signi cant ($p < 0.01$) negative correlations with monthly February and August, seasonal June–August, and the annual sum are obtained using MXD.

A similar relationship between radial growth and climate of several *Pinus uncinata* TRW (near timberline) sites from the Central Spanish Pyrenees has been observed (Tardif et al. 2003). For more details on the growth/climate

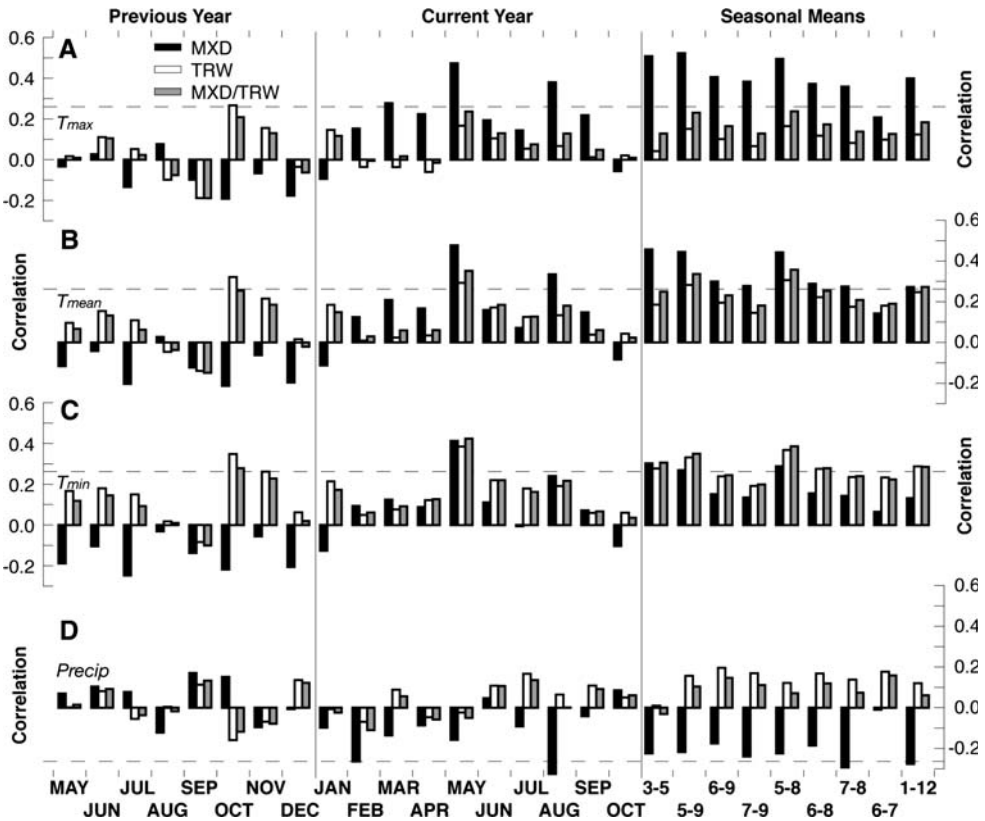

Fig. 6 Growth/climate response of the MXD (*black*), TRW (*white*), and their mean (*grey*) RCS chronologies using a maximum temperatures, b mean temperatures, c minimum temperatures, and d precipitation sums. Correlations are computed from previous year May to current year October over the common 1901–2002 period. *Horizontal dashed lines* denote the 99% signi cance levels, corrected for *lag-1* autocorrelation. Temperature data are derived from the Pic du Midi station, and precipitation data from the CRUTS2.1 dataset, using the mean of 15 grid-boxes that cover 0–2E and 42–43N. Numbers on *x*-axis refer to March–May, May–September, June–September, July–September, May–August, June–August, July–August, June–July, and January–December, respectively

response of various tree-ring parameters in the Pyrenees (see Büntgen et al. 2007b). A distinct response optimum of MXD to maximum growing season temperatures is found in British Columbia, Canada (Luckman and Wilson 2005; Wilson and Luckman 2003), and also in the Altai Mountains, southern Russia (Frank et al. 2007a). Comparable patterns of MXD formation, i.e., strong correlation with temperature during the early and late vegetation period with weaker correlation in between, are reported from a high-elevation larch network in the Swiss Alps (Büntgen et al. 2006b), from a multi-species network across the greater Alpine region (Frank and Esper 2005a), and from hundreds of sites along the northern latitudinal timberline (Briffa et al. 2002). Some altitudinal/latitudinal modi cation of the absolute growing season length, however, should be taken into account, when comparing results from such different geographical regions.

3.3 Temperature reconstruction

May–September minimum, mean and maximum temperatures from the Pic du Midi station together with mean temperatures from the corresponding 5×5.0 HadCRUT3v and 0.5× 0.5 CRUTS2.1 grid-boxes were analyzed to emphasize potential uncertainty within the meteorological 'target' data (Fig. 7). Note that measurements from the Pic du Midi are not included in both grid-sets. After * 1945, the ve records show similar behavior, with higher (lower) agreement in the high (low) frequency domain. An earlier offset, particularly between the minimum and maximum values, but also between the various sources is most evident for the longer-term trends (Fig. 7a). A similar offset between warmer maximum and cooler minimum temperatures before * 1900 is reported from a network of 22 instrumental stations across the Iberian Peninsula (Brunet et al. 2006). Linear trends computed over the common 1901–2002 period range from − 0.4 C (HadCRUT3v; mean temp.) to 1.5 C (Pic du Midi; min. temp.). Maximum temperatures from the Pic du Midi show no longer-term warming, whereas minimum values increased from 1882 onwards, resulting in a decline of the mean annual diurnal temperature range, with all seasons being affected. Changes in the observed night- and day-time values are most likely related to changes in relative humidity, cloud cover, and related greenhouse effects. The overall uncertainty range in station measurements is, however, minimized towards the end of the twentieth century (Dessens and Bücher 1995). Thirty-one year moving inter-series correlations between the ve temperature records emphasize increased coherency towards present, which is independent of the frequency domain used (Fig. 7c). The decline in inter-series correlation is most evident for the low-passed data and during the rst half of the last century. Different trends between the various meteorological records prior to* 1945 make the statistical

Fig. 7 a Comparison between unfiltered and 15-year low-pass filtered May–September minimum, mean, and maximum temperatures from the Pic du Midi station (*blue, green, and red*), and mean temperatures from the corresponding CRUTS2.1 (Mitchell and Jones 2005) and HadCRUT3v (Brohan et al. 2006) grids (*black and gray*). b Comparison between the 15-year high-pass components c 31-year moving inter-series correlations between the five individual series. Values are expressed as anomalies with respect to the 1961–1990 period and records smoothed using cubic smoothing spline functions

differentiation and selection of the proper 'target' data exceptionally challenging. Various examples for a similar decoupling between generally warmer instrumental measurements of Alpine summer temperature before ~1860 compared to colder tree-ring estimates are reviewed in Frank et al. (2007c).

Due to potential uncertainty in the meteorological data during the first half of the twentieth century, we calibrated the PYR chronology over the 1944–2005 period and against maximum May–September temperatures from the Pic du Midi (Fig. 8a). The chronology explains 29% of the temperature data during this calibration period, 27% over the full 1882–2005 period of proxy/target overlap, and 24% over the 1882–1943 verification period. After regressing the proxy against instrumental temperatures over the 1944–2005 calibration period, RE and CE values of the corresponding 1882–1943 period of verification are 0.24 and 0.18, respectively. Similarly, RE and CE values of 0.25 and 0.28 are retained after flipping the periods and using 1944–2005 for verification. Although there is no significance test, as a 'rule of thumb', values >0 (with RE > CE) indicate some useful information in the regression reconstruction (Cook et al. 1994). However, to avoid loss of amplitude due to regression error (Esper et al. 2005a), a simple scaling of the MXD chronology to the meteorological data was additionally applied, i.e., the variance and mean of the proxy record were set equal to those of the instrumental data. Residuals between actual and scaled values show no trend over the full 1882–2005 period of proxy/target overlap (Fig. 8b), suggesting that there is no systematic lower frequency divergence that could potentially arise from the application of RCS detrending (Melvin 2004). After dividing tree-ring and instrumental data into 15-year high- and low-pass components (Fig. 8c, d), correlations illustrate that the amount of unexplained proxy/target variability is mainly restricted to the lower frequency domain. The chronology shows highest correlation with inter-annual variations of warm season maximum temperatures. This coherency most likely results from the fact that maximum daily temperatures are the main controlling growth factor at our sites. Moving 31-year correlations between the actual and modeled maximum temperatures are significant ($p < 0.01$) from ~1970 to present, whereas less coherency is indicated prior to 1970 (Fig. 8e). Moving 31-year correlations between the actual and modeled 15-year high-pass components are, however, constantly significant ($p < 0.01$) back to ~1940, and around 1920. As the modeled temperature signal is strong at higher frequencies (<15 years) and as the residuals between MXD and instrumental data show no trend, we assume some useful temperature information to be preserved.

Common features between the measured and estimated maximum May–September temperatures include relatively stable temperatures from ~1880 to 1950, a decrease from ~1950 to 1980, and a most recent increase from ~1980 to present. No anomalous and systematic divergence between (warmer) actual and (cooler) estimated temperatures during the past decades, as reported from some tree-ring sites in the Alps (Büntgen et al. 2006a), and across the northern latitudes (Briffa et al. 1998), for example, is observed. This ability of tracking the most recent summer warmth is in line with revised network analyses from the Alpine arc (Büntgen et al. 2008).

As an additional comparison of the new PYR reconstruction, we utilized the average of the nearest grid-points (0–1.5 E; 41–43 N) of the multi-proxy EU June-August temperature reconstructions (1500–2002) derived from

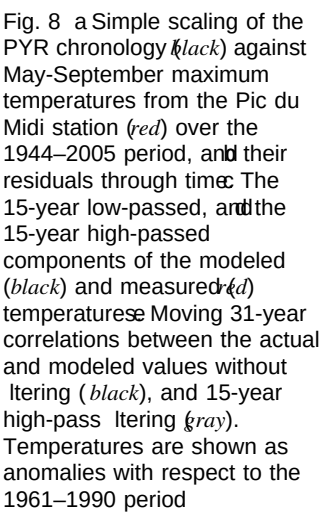

Fig. 8 a Simple scaling of the PYR chronology (*black*) against May-September maximum temperatures from the Pic du Midi station (*red*) over the 1944–2005 period, and b their residuals through time. c The 15-year low-passed, and d the 15-year high-passed components of the modeled (*black*) and measured (*red*) temperatures. e Moving 31-year correlations between the actual and modeled values without filtering (*black*), and 15-year high-pass filtering (*gray*). Temperatures are shown as anomalies with respect to the 1961–1990 period

Luterbacher et al. (2004). A significant correlation (at the 99.9% level) was revealed throughout the last 500 years. Higher correlations of the post 1750 period and lower ones before might result from increasing uncertainties in both reconstructions back in time.

Uncertainty in the PYR record is most evident on decadal time-scales. Potential sources of bias include: (1) Relict material from both sampling sites becomes exceptionally scarce in the thirteenth century, causing insufficient chronology replication prior to AD 1260. (2) Variable degrees of relict wood decay can influence the stem coring location, introducing deviations from the standard sampling location at breast height, and thus hinder the estimation of germination ages. (3) The overall long-term 'shape' of RCS chronologies is somewhat insecure (i.e., relative level of the recent warmth compared to conditions during the records earliest portion), as various implications of data and methodology are not yet fully quantified (Esper et al. 2003; Helama et al. 2005; Melvin 2004). (4) A limited number of 'proper' (i.e., length, homogenization, parameter) instrumental station data that reflect climate conditions of the high-elevation sampling sites, hampers calibration/verification trials to be performed over longer intervals.

3.4 Temporal variability

The newly developed PYR temperature reconstruction is compared with millennium-long records from the central Alps and northern Scandinavia to assess patterns of past EU summer temperature variability (Fig. 9a). All three records are exclusively based on MXD measurements, used the RCS method for series detrending, and were calibrated against best-fit summer temperatures (Table 1b). The PYR record indicates relatively cold temperatures during the late thirteenth century, followed by a century of generally warmer summers centered * 1400, and pronounced cooling from * 1500 to 1850. Temperatures over the past * 200 years generally increased with some decadal fluctuations such as the 1810–1920s and 1960–1970s. The Alpine temperature history reports warm summers during much of the twelfth and late thirteenth centuries commonly associated with the late MWP, followed by a prolonged cooling until * 1700, and generally rising temperatures until 2003. A different temperature course is reconstructed for northern Scandinavia. After a cold thirteenth century, relatively warm summers occurred from * 1300 until the end of the sixteenth century, followed by rather cold conditions over the past four centuries, interrupted by warming in the late eighteenth and twentieth centuries. All three reconstructions provide evidence for cold conditions during the Maunder (1645–1715), and Dalton (1790–1820) solar minima (Eddy 1976), with physical explanations being provided elsewhere (e.g., Foukal et al. 2006). The later cooling phase was most likely amplified by the radiative effect following the Tambora/Indonesia volcanic eruption in April 1815 (Oppenheimer 2003). While Alpine temperatures increased constantly after 1710 until the present, temperatures reconstructed for the Pyrenees did

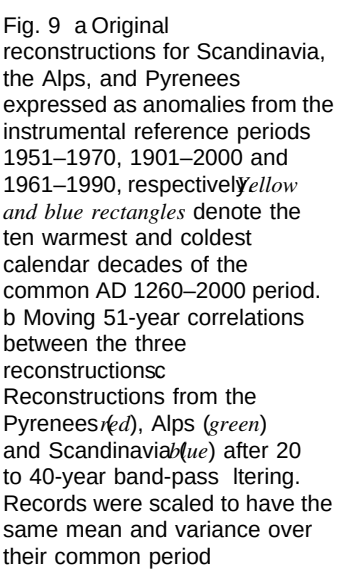

Fig. 9 a Original reconstructions for Scandinavia, the Alps, and Pyrenees expressed as anomalies from the instrumental reference periods 1951–1970, 1901–2000 and 1961–1990, respectively. *Yellow and blue rectangles* denote the ten warmest and coldest calendar decades of the common AD 1260–2000 period. b Moving 51-year correlations between the three reconstructions. c Reconstructions from the Pyrenees (*red*), Alps (*green*) and Scandinavia (*blue*) after 20 to 40-year band-pass filtering. Records were scaled to have the same mean and variance over their common period

not start increasing before the 1830, but describe a comparable decline for the 1970s, followed by the most recent warming trend. Long-term temperature changes in northern Sweden diverge considerably from those reported for the Alps and Pyrenees, as warmest summers occurred in the 1760s, followed by two centuries of relatively cold conditions. The post 1970s warmth is also reflected by the Torneträsk data (see Grudd 2008 for details).

Commonly reported ups and downs in-phase with the so-called LIA Type Events—a term introduced by Wanner et al. (2000)—most likely refer to modifications in atmospheric circulation patterns during the Wolf (1290–1320), Maunder and Dalton solar minima (Luterbacher et al. 2001, 2002; Wanner et al. 1997; Xoplaki et al. 2001). The latter (~1850) is associated with the most extended Alpine Holocene glaciers advance (e.g., Holzhauser et al. 2005). Interestingly, most Scandinavian glaciers reached their late Holocene maximum during the early to mid 18th century (Nesje and Dahl 2003 and references therein), and glaciers in northern Sweden and Norway, mostly those located on the more continentally influenced eastern slope of the Scandes, advanced until the beginning of the twentieth century (Karlén 1988). Besides such local-scale variation in late Holocene glacier fluctuations across Scandinavia, causes for asynchronous LIA maxima between the Alps and Scandinavia remain unclear. Since rapid fluctuations in mass-balance, particularly of maritime glaciers in western Scandinavia, are driven in part by winter precipitation (Nesje et al. 2000), caution is advised when comparing such archives with tree-ring based summer temperature reconstructions.

Moving 51-year correlations between the three reconstructions show relatively high coherency between the Alps and Pyrenees back to 1450, whereas correlations with the Scandinavian data are generally lower and temporally unstable (Fig. 9b). Over the AD 1260–2003 common period, the correlation between the Pyrenees and Alps is 0.34, remains the same after 40-year high-pass filtering, but increases to 0.41 and 0.57 after 40-year low-pass and 20–40 year band-pass filtering, respectively (Fig. 9c). Non-significant correlations are found between Scandinavia and either the Alps or the Pyrenees. The strongest agreement between the Pyrenees and Alps is obtained on the mid-frequency domain, likely due to a combination of the proxy's unexplained variance in longer-term fluctuations, plus some regional-induced differences in the preserved high-frequency signal. Correlation between the Pyrenees and Alpine proxy data is 0.45 over the 1882–2003 period.

Correlation between the instrumental target data from these regions is 0.51 over the same period. Correlation between the Scandinavian reconstruction and records from the Alps and Pyrenees is 0.11 and 0.01, respectively (1882–2003). Interestingly, similarly low correlations of 0.14 and 0.06 are obtained when using the Scandinavian instrumental targets and those from the Alps and Pyrenees, respectively.

3.5 Spatial variability

Spatial correlations between the three regional-scale reconstructions and gridded surface temperature data reveal distinct clusters indicating each record's geographical representation, including apparent boundaries and gradients of EU-scale climate variability (Fig. 10). The Torneträsk data are associated with a temperature field north of approximately 50–55° latitude with a large east-west extension. The field denoted by the Alpine data is restricted to the region south of 50° latitude, with the core region being much smaller. The temperature field represented by the Pyrenees data shows generally lower correlations compared to those derived for Scandinavia and the Alps, and partly overlaps with the Alpine pattern. While the Pyrenees reconstruction best reflects maximum temperatures, the gridded data represent mean temperatures, an offset likely introducing some bias. There is no spatial overlap between the northern Scandinavian and central Alpine clusters as previously stressed by missing coherence between the reconstructed time-series back to AD 1260. In contrast, the Pyrenees and Alpine clusters partly overlap. For interpretation and validation of the proxy-based spatial field correlations, similar maps were computed using the corresponding meteorological 'target' data over the 1882–2003 period. While the Scandinavian spatial field of correlations is basically resembled, slight differences are found for the Alps and Pyrenees. Highest values of the Alpine spatial field of correlation now describe a greater region, most likely due to the larger spatial coverage of the high-elevation instrumental mean applied. The Pyrenees spatial field is more distinct

Fig. 10 *Left hand side* shows spatial correlations between the temperature reconstructions from a Torneträsk (northern Sweden), b Valais (Swiss Alps), and c Pyrenees (Central Spanish Pyrenees), and the gridded 5 × 5° HadCRUT3v dataset of monthly surface temperatures (Brohan et al. 2006). *Right hand side* shows the corresponding results for the meteorological records used for calibration at Northern Sweden, b high-elevation Alps, and c Pic du Midi. Black stars indicate the locations of the records. Insets denote reconstructed (*left*) and measured (*right*) time-series utilized for correlation over the common 1850–2003 and 1882–2003 period, respectively

compared to the Alps, with highest correlations southwest of the station location.

Overall, the three regional patterns of spatial field correlations as derived from either the proxy or instrumental data are similar. A clear synoptic separation between northern Scandinavia and central EU is emphasized, whereas the greater Alpine region and Mediterranean basin are both influenced by the same synoptic regimes. These results are consistent for various frequency bands and time periods. See Raible et al. (2006) and Xoplaki et al. (2003, 2004) for a detailed description of long-term EU climate variability derived from instrumental observations, proxy reconstructions, and model simulations.

Synoptic-scale circulation types were additionally evaluated using reconstructed fields of gridded 500 hPa geopotential height data back to 1659 (Luterbacher et al. 2002). A composite technique revealed the dominant mid-troposphere pressure systems triggering the 34 (equal 10%) coldest and warmest years over the common period 1659–1999 (Fig. 11). While a significant ($p < 0.01$) low-pressure anomaly (with respect to the 1659–1999 mean) over central EU is fund to be the principal mode during coldest years, a less distinct high-pressure cell above the Mediterranean basin triggers regional warm spells. Interestingly, the low-pressure deviation (−15 to 7) is more pronounced in comparison to the positive departure (−8 to 7), indicating more skill in the reconstruction of cold summer extremes. Similar results from the Alps demonstrate advanced ability in capturing annual negative (cold) extremes but a slight underestimation of positive (warm) extremes (Büntgen et al. 2006b).

3.6 Large-scale comparison

Large-scale temperature reconstructions are considered to link patterns of past EU climate variations with those reconstructed for the NH (Fig. 12a, b). This concert of approaches (Briffa 2000; D'Arrigo et al. 2006; Esper et al. 2002; Jones et al. 1998; Mann et al. 1999; Moberg et al. 2005) reveals an overall centennial to longer-scale common signal, but shows relative level differences for the MWP, LIA and recent warmth (Esper et al. 2005b). Reasons for similarities and dissimilarities between these reconstructions are discussed elsewhere (Esper 2004; Mann et al. 2005; Rutherford et al. 2005). Besides other data overlap, TRW measurements from Swedish Torneträsk were used in each of the six large-scale records, with its relative weight increasing back in time, as only few data are available before AD 1400 (D'Arrigo et al. 2006). No data overlap between the NH records and the newly developed Pyrenees and Alpine reconstructions exists. Correlations between the regional- and large-scale records describe a generally lower agreement for the unfiltered data, but increasing coherence after 20- and 40-year low-pass filtering (Fig. 12c). Highest (lowest) correlations were found for the 40-year smoothed Alpine (Scandinavian) and NH multi-proxy reconstruction by Moberg et al. (2005). While correlations between the unfiltered Pyrenees and the NH reconstructions are mostly lower than those obtained from the Alpine and Scandinavian records, relative strong correlations derive from the smoothed Pyrenees time-series. Mean 51-year moving correlations between the three regional- and six large-scale reconstructions indicate increasing agreement about AD 1500 (not shown). While mean correlations between the Alpine and Scandinavian data, and the NH records are generally similar, increased coherency between the Scandinavian and NH records is found around AD 1050–1450, likely due to the increased importance of data overlap. Moving correlations between the new Pyrenees and the NH reconstructions are commonly lower than those of the Scandinavian and Alpine records. Reasons are manifold and include the lower explained variance of the Pyrenees record, the higher explained variance of the Alpine record, the greater data overlap with the Scandinavian record, and the differing latitudinal representation of the data.

The Scandinavian and Alpine reconstructions, in-phase with the NH records generally portray high temperatures centered * 1000 (Fig. 9). Low values during the Oort solar minimum * 1040 to 1080 are most evident in the Alpine, and partly in the NH records (Fig. 12). Relatively high temperatures in the second half of the twelfth century are

Fig. 11 Composite analysis between the new regional-scale summer temperature history of the Pyrenees and the European-scale reconstruction of 500 hPa geopotential height by Luterbacher et al. (2002), using the 34 (a) coldest and (b) warmest years (1659–1999). The *black star* indicates the location of this study, and the *black lines* are bootstrap significance levels

Fig. 12 Comparison between 20-year low-pass filtered a regional and b Northern Hemisphere temperature reconstructions scaled to have the same mean and variance over the AD 1260–2003, and 1000–1979 period, respectively. c Correlations (1260–1979) between the unfiltered and smoothed regional- and large-scale records

common to all reconstructions, although decadal-scale divergence during that early period is evident. While the Scandinavian, Pyrenees and NH reconstructions indicate low temperatures for the second half of the thirteenth century those estimated for the Alpine region are relatively warm. Temperatures during the sixteenth century are estimated to be warm in Scandinavia, cold in the Alps, and about average in the Pyrenees and NH records. A prolonged period of cold summers from 1600 to 1850 is most evident in the Pyrenees and Alps, with comparable values seen in the NH records. While warmest summers in the Alps, Pyrenees, and the NH are documented for the twentieth century, Scandinavian summers are reconstructed to be about average during that period. The depression of 1970 prior to the most recent warming is distinct for the Pyrenees and Alps, but less pronounced in Scandinavia. None of the NH reconstructions allows the most recent decade of warming (e.g., Brohan et al. 2006) to be placed in a longer-term context, as records end between 1979 and 1996. The dominance of TRW data further complicates benchmarking climatic extremes, as annual variations in TRW reflect a shorter portion of the high summer season with a tendency of containing some effects of the previous year climate. In contrast, variations in MXD capture temperatures of an extended season with reduced biological persistence (e.g., Frank and Esper 2005a).

4 Conclusions

Our collection of living and dry-dead wood from two timberline sites in the Central Spanish Pyrenees results in a composite dataset spanning the AD 924–2005 period. Two chronologies developed on a site-by-site basis correlate at 0.57 over the 1517–2005 common period. The new Pyrenees chronology correlates at 0.53 with maximum May–September temperatures from the Pic du Midi (1944–2005). The common signal is weighted towards higher frequency variations, as correlation increases to 0.68 after 15-year high-pass filtering. The final reconstruction covers the 1260–2005 period and reveals relatively high temperatures in the 14–15th and twentieth century, separated by a rather prolonged cooling from 1450 to 1850. The six warmest decades occurred during the twentieth century, with the following four being reconstructed for the period 1360–1440. Comparison with summer temperature reconstructions from the Swiss Alps and northern Scandinavia indicates decadal to longer-term similarity between the Pyrenees and Alps, but notable independence for northern EU. Twentieth century warmth is evident in the Alps and Pyrenees, whereas Scandinavian temperatures are relatively cold compared to those centered on 1000, 1400 and 1750. Temperature depressions during the second half of the fifteenth century, between 1600 to 1700, and 1820 are common features of all reconstructions. Lowest temperatures in Scandinavia, however, occurred at the onset of the twentieth century. Spatial field correlations using proxy and target data reveal similar patterns. Both describe a distinct separation between the northern Scandinavian and Alpine spatial fields of correlations, but significant overlap of the Alpine and Pyrenees clusters. Comparison of the three regional-scale studies with six large-scale records suggests that decadal-scale fluctuations of EU summer temperatures are fairly synchronous with those reported

from the NH, i.e., common decadal-scale depressions occurred around* 1350, 1460, 1600, 1700, 1820, and 1970. The Pyrenees MXD record lls a spatial gap in the worldwide tree-ring density network. This gap happens to coincide with lower latitudes, which are generally under-represented in terms of long-term temperature data. The new reconstruction improves our understanding of past EU temperature variations, and will contribute to the enhancement of NH tree-ring compilations.

The comparison of the three MXD-based summer temperature reconstructions shows divergence in their long-term variations, which allows spatiotemporal patterns in past EU temperatures to be distinguished. These regional discrepancies further indicate the complexity of continental-scale climate variability. Therefore, future research will need to consider (1) the update of existing (e.g., covering the entire Pyrenees from the Mediterranean Sea in the east to the Atlantic Ocean in the west), and (2) development of new regional-scale composite chronologies (e.g., providing tree-ring evidence from the Carpathian arc). Such data should exclusively be derived from (3) high-elevation timberline sites, containing (4) relict and sub-fossil wood, and with (5) MXD measurements being performed.

Acknowledgments We thank F.H. Schweingruber for site selection, the National Park d'Aigüestortes I Estany de Sant Maurici (Jordi Vicente i Canillas) for sampling permission and logistic support, R.J.S. Wilson for eld assistance and discussion. J. Dessens kindly provided instrumental data from the Pic du Midi. Spatial eld correlations were generated using the KNMI Climate Explorer (http://www.climexp.knmi.nl). Supported by the SNF project NCCR-Climate and Euro-Trans (#200021-105663), and the EU project Millennium (#017008-2).

References

Auer I, and 31 co-authors (2007) HISTALP—Historical instrumental climatological surface time series of the greater Alpine region 1760–2003. Int J Climatol 27:17–46

Brázdil R, P ster C, Wanner H, von Storch H, Luterbacher J (2005) Historical climatology in Europe—state of the art. Clim Change 70:363–430

Briffa KR (2000) Annual climate variability in the Holocene: interpreting the message of ancient trees. Q Sci Rev 19:87–105

Briffa KR, Jones PD, Bartholin TS, Eckstein D, Schweingruber FH, Karlén W, Zetterberg P, Eronen M (1992) Fennoscandian summers from AD 500: temperature changes on short and long timescales. Clim Dyn 7:111–119

Briffa KR, Jones PD, Schweingruber FH, Shiyatov SG, Cook ER (1995) Unusual twentieth-century summer warmth in a 1000-year temperature record from Sibiria. Nature 376:156–159

Briffa KR, Jones PD, Schweingruber FH, Osborn TJ (1998) In uence of volcanic eruptions on Northern Hemisphere summer temperature over the past 600 years. Nature 393:450–455

Briffa KR, Osborn TJ, Schweingruber FH, Jones PD, Shiyatov SG, Vaganov EA (2002) Tree-ring width and density around the Northern Hemisphere: Part 1, local and regional climate signals Holocene 12:737–757

Briffa KR, Shishov VV, Melvin TM, Vaganov EA, Grudd H, Hantemirov RM, Eronen M, Naurzbaev MM (2007) Trends in recent temperature and radial tree growth spanning 2000 years across northwestern Eurasia. Philos Trans Roy Soc B. doi: 10.1098/rstb.2007.2199

Brohan P, Kennedy JJ, Harris I, Tett SFB, Jones PD (2006) Uncertainty estimates in regional and global observed temperature changes: a new dataset from 1850. J Geophys Res 111:D12106. doi:10.1029/2005JD006548

Brunet M, Saladie O, Jones P, Sigró J, Aguilar E, Moberg A, Lister D, Walther A, Lopez D, Almarza C (2006) The development of a new dataset of Spanish daily adjusted temperature series (SDATS) (1850–2003). Int J Clim 26:1777–1802

Bücher A, Dessens J (1991) Secular trend of surface temperature at an elevated observatory in the Pyrenees. J Clim 4:859–868

Büntgen U, Esper J, Frank DC, Nicolussi K, Schmidhalter M (2005) A 1052-year tree-ring proxy of Alpine summer temperatures. Clim Dyn 25:141–153

Büntgen U, Frank DC, Schmidhalter M, Neuwirth B, Seifert M, Esper J (2006a) Growth/climate response shift in a long subalpine spruce chronology. Trees Struct Funct 20:99–110

Büntgen U, Frank DC, Nievergelt D, Esper J (2006b) Summer temperature variations in the European Alps, AD 755–2004. J Clim 19:5606–5623

Büntgen U, Bellwald I, Kalbermatten H, Schmidhalter M, Freund H, Frank DC, Bellwald W, Neuwirth B, Nüsser M, Esper J (2006c) 700 years of settlement and building history in the Lötschental/Switzerland. Erdkunde 60/2:96–112

Büntgen U, Frank DC, Kaczka RJ, Verstege A, Zwijacz-Kozica T, Esper J (2007a) Growth/climate response of a multi-species tree-ring network in the Western Carpathian Tatra Mountains, Poland and Slovakia. Tree Physiol 27:689–702

Büntgen U, Frank DC, Verstege A, Nievergelt D, Esper J (2007b) Climatic response of multiple tree-ring parameters from the Central Spanish Pyrenees. Trace 5:60–72

Büntgen U, Frank DC, Wilson R, Esper J (2008) Testing for tree-ring divergence in the European Alps. Global Change Biol (in press)

Camarero JJ, Guerrero-Campo J, Gutiérrez E (1998) Tree-ring growth and structure of Pinus uncinata and Pinus sylvestris in the Central Spanish Pyrenees. Arctic Alpine Res 30:1–10

Casty C, Wanner H, Luterbacher J, Esper J, Böhm R (2005) Temperature and precipitation variability in the European Alps since 1500. Int J Climatol 25:1855–1880

Cook ER (1985) A time series analysis approach to tree-ring standardization. PhD Thesis, University of Arizona, pp 171

Cook ER, Peters K (1981) The smoothing spline: A new approach to standardizing forest interior tree-ring width series for dendroclimatic studies. Tree-Ring Bull 41:45–53

Cook ER, Briffa KR, Jones PD (1994) Spatial regression methods in dendroclimatology: a review and comparison of two techniques. Int J Climatol 14:379–402

Cook ER, Briffa KR, Meko DM, Graybill DA, Funkhouser G (1995) The 'segment length curse' in long tree-ring chronology development for palaeoclimatic studies. Holocene 5:229–237

D'Arrigo R, Wilson RJS, Jacoby GC (2006) On the long-term context for late 20th century warming. J Geophys Res 111:D03103. doi: 10.1029/2005JD006352

Dessens J, Bücher A (1995) Changes in minimum and maximum temperatures at the Pic du Midi in relation with humidity and cloudiness, 1882–1984. Atmos Res 37:147–162

Dessens J, Bücher A (1997) A critical examination of the precipitation records at the Pic du Midi observatory, Pyrenees, France. Clim Change 36:345–353

Eddy JA (1976) The Maunder minimum. Science 192:1189–1202

Efron B (1987) Better bootstrap con dence intervals. J Am Stat Assoc 82:171–185

Esper J, Cook ER, Schweingruber FH (2002) Low-frequency signals in long tree-ring chronologies for reconstructing past temperature variability. Science 295:2250–2252

Esper J, Cook ER, Krusic PJ, Peters K, Schweingruber FH (2003) Tests of the RCS method for preserving low-frequency variability in long tree-ring chronologies. Tree-Ring Res 59:81–98

Esper J, Frank DC, Wilson RJS (2004) Low frequency ambition, high frequency ration. EOS 85:113–120

Esper J, Frank DC, Wilson RJS, Briffa KR (2005a) Effect of scaling and regression on reconstructed temperature amplitude for the past millennium. Geophys Res Lett 31. doi:10.1029/2004GL021236

Esper J, Wilson RJS, Frank DC, Moberg A, Wanner H, Luterbacher J (2005b) Climate: past ranges and future changes. Q Sci Rev 24:2164–2166

Esper J, Frank DC, Büntgen U, Verstege A, Luterbacher J, Xoplaki E (2007) Long-term drought severity variations in Morocco. Geophys Res Lett 34. doi:10.1029/2007GL030844

Foukal P, Fröhlich C, Spruit H, Wigley TML (2006) Variations in solar luminosity and their effect on the Earth's climate. Nature 433:161–166

Frank DC, Esper J (2005a) Characterization and climate response patterns of a high elevation, multi species tree-ring network for the European Alps. Dendrochronologia 22:107–121

Frank DC, Esper J (2005b) Temperature reconstructions and comparisons with instrumental data from a tree-ring network for the European Alps. Int J Climatol 25:1437–1454

Frank DC, Ovchinnikov D, Kirdyanov A, Esper J (2007a) The potential for long-term climatic reconstructions in the Central Altay Mountains from living and relict larch. Trace 5:85–96

Frank DC, Esper J, Cook E (2007b) Adjustment for proxy number and coherence in a large-scale temperature reconstruction. Geophys Res Lett 34. doi:10.1029/2007GL030571

Frank DC, Büntgen U, Böhm R, Maugeri M, Esper J (2007c) Warmer early instrumental measurements versus colder reconstructed temperatures: shooting at a moving target. Q Sci Rev. doi:10.1016/j.quascirev.2007.08.002

Fritts HC (1976) Tree rings and climate. Academic Press, London, pp 567

Grove JM (1988) The little ice age. Methuen & Co., London, New York, pp 498

Grudd H, Briffa KR, Karlén W, Bartholin TS, Jones PD, Kromer B (2002) A 7400-year tree-ring chronology in northern Swedish Lapland: natural climatic variability expressed on annual to millennial timescales. Holocene 12:657–665

Grudd H (2008) Torneträsk tree-ring width and density AD 500–2004: a test of climatic sensitivity and a new 1500-year reconstruction of northern Fennoscandian summers. Clim Dyn. doi:10.1007/s00382-007-0358-2

Gutiérrez E (1991) Climatic tree growth relationships for Pinus uncinata Ram. in the Spanish pre-Pyrenees. Act Oecol 12:213–225

Hegerl GC, Crowley TJ, Hyde WT, Frame DJ (2006) Climate sensitivity constrained by temperature reconstructions over the past seven centuries. Nature 440:1029–1032

Helama S, Timonen M, Lindholm M, Merilainen J, Eronen M (2005) Extracting long-period climate fluctuations from tree-ring chronologies over timescales of centuries to millennia. Int J Climatol 25:1767–1779

Holzhauser H, Magny M, Zumbühl HJ (2005) Glacier and lake-level variations in west-central Europe over the last 3500 years. Holocene 15:789–801

Jones PD, Briffa KR, Barnett TP, Tett SFB (1998) High-resolution palaeoclimatic records for the past millennium: interpretation, integration and comparison with general circulation model control-run temperatures. Holocene 8:455–471

Karlén W (1988) Scandinavian glacial and climate fluctuations during the Holocene. Q Sci Rev 7:199–206

Lamb HH (1965) The early medieval warm epoch and its sequel. Palaeogeogr Palaeoclimatol Palaeoecol 1:13–37

Luckman BH, Wilson RJS (2005) Summer temperatures in the Canadian Rockies during the last millennium: a revised record. Clim Dyn 24:131–144

Luterbacher J, Rickli R, Xoplaki E, Tinguely C, Beck C, Pfister C, Wanner H (2001) The late Maunder Minimum (1675–1715)—a key period for studying decadal scale climate change in Europe. Clim Change 49:441–462

Luterbacher J, Xoplaki E, Dietrich D, Jones PD, Davies TD, Portis D, Gonzalez-Rouco JF, von Stroch H, Gyalistras D, Casty C, Wanner H (2002) Extending North Atlantic Oscillation reconstructions back to 1500. Atmos Sci Lett 2:114–124

Luterbacher J, Dietrich D, Xoplaki E, Grosjean M, Wanner H (2004) European seasonal and annual temperature variability, trends and extremes since 1500 A.D. Science 303:1499–1503

Luterbacher J, 48 co-authors (2006) Mediterranean climate variability over the last centuries: A review. In: Lionello P, Malanotte-Rizzoli P, Boscolo R (eds) The Mediterranean Climate: an overview of the main characteristics, issues. Elsevier, Amsterdam, pp 27–148

Mann ME, Bradley RS, Hughes MK (1999) Northern Hemisphere temperatures during the past millennium—inferences, uncertainties, and limitations. Geophys Res Lett 26:759–762

Mann ME, Rutherford S, Wahl E, Ammann C (2005) Testing the fidelity of methods used in proxy-based reconstructions of past climate. J Clim 18:4097–4106

Melvin TM (2004) Historical growth rates and changing climatic sensitivity of boreal conifers. PhD Thesis, Climatic Research Unit, School of Environmental Sciences, University of East Anglia, 271 pp

Mitchell TD, Jones PD (2005) An improved method of constructing a database of monthly climate observations and associated high-resolution grids. Int J Climatol 25:693–712

Moberg A, Sonechkin DM, Holmgren K, Datsenko NM, Karlén W (2005) Highly variable Northern Hemisphere temperatures reconstructed from low- and high-resolution proxy data. Nature 433:613–617

Nesje A, Lie Ø, Dahl SO (2000) Is the North Atlantic Oscillation reflected in Scandinavian glacier mass balance records? J Quat Sci 15:587–601

Nesje A, Dahl SO (2003) The 'Little Ice Age'—only temperature? Holocene 13:139–145

Nicolussi K, Patzelt G (2000) Discovery of early Holocene wood and peat on the forefield of the Pasterze Glacier, Eastern Alps, Austria. Holocene 10:191–199

Oppenheimer C (2003) Climatic, environmental and human consequences of the largest known historic eruption: Tambora volcano (Indonesia) 1815. Prog Phys Geogr 27/2:230–259

Osborn TJ, Briffa KR, Jones PD (1997) Adjusting variance for sample-size in tree-ring chronologies and other regional-mean time-series. Dendrochronologia 15:89–99

Pauling A, Luterbacher J, Casty C, Wanner H (2006) 500 years of gridded high resolution precipitation reconstructions over Europe and the connection to large-scale circulation. Clim Dyn 26:387–405

Pla S, Catalan J (2005) Chrysophyte cysts from lake sediments reveal the submillennial winter/spring climate variability in the northwestern Mediterranean region throughout the Holocene. Clim Dyn 24:263–278

Raible CC, Casty C, Luterbacher J, Pauling A, Esper J, Frank DC, Büntgen U, Roesch AC, Tschuck P, Wild M, Vidale PL, Schär C, Wanner H (2006) Climate variability - observations, reconstructions, and model simulations for the Atlantic-European and

Alpine region from 1500–2100 AD. Clim Change. doi: 10.1007/s10584-006-9061-2
Rolland C, Schueller F (1994) Relationships between mountain pine and climate in the French Pyrenees (Font-Romeu) studied using the radiodensitometrical method. Pirineos 144:55–70
Ruiz-Flaño P (1988) Dendroclimatic series of *Pinus uncinata* R. in the Central Pyrenees and in the Iberian System. A comparative study. Pirineos 132:49–64
Rutherford S, Mann ME, Osborn TJ, Bradley RS, Briffa KR, Hughes MK, Jones PD (2005) Proxy based northern hemisphere surface temperature reconstructions: sensitivity to methodology, predictor network, target season, and target domain. J Clim 18:2308–2329
Szeicz JM, MacDonald GM (1995) Dendroclimatic reconstruction of summer temperatures in Northwestern Canada Since A.D. 1638 based on age dependent modelling. Q Res 44:257–266
Schär C, Vidale PL, Lüthi D, Frei C, Häberli C, Liniger MA, Appenzeller C (2004) The role of increasing temperature variability in European summer heatwaves. Nature 427:332–336
Schweingruber FH, Bartholin T, Schär E, Briffa KR (1988) Radiodensitometric-dendroclimatological conifer chronologies from Lapland (Scandinavia) and the Alps (Switzerland). Boreas 17:559–566
Tardif J, Camarero JJ, Ribas M, Gutiérrez E (2003) Spatiotemporal variability in tree growth in the Central Pyrenees: climatic and site influences. Ecol Monogr 73:241–257
Trenberth K (1984) Some effects of finite sample size and persistence on meteorological statistics. Part I: Autocorrelations. Mon Weath Rev 112:2359–2368
Wang L, Payette S, Bégin Y (2001) 1300-year tree-ring width and density series based on living, dead and subfossil black spruce at tree-line in Subarctic Québec, Canada. Holocene 11:333–341
Wanner H, Holzhauser H, Pfister C, Zumbühl H (2000) Interannual to century scale climate variability in the European Alps. Erdkunde 54:62–69
Wanner H, Rickli R, Salvisberg E, Schmutz C, Schüpp M (1997) Global climate change and variability and its influence on alpine climate—concepts and observations. Theor Appl Climatol 58:221–243
Wigley TML, Briffa KR, Jones PD (1984) On the average of value of correlated time series, with applications in dendroclimatology and hydrometeorology. J Clim Appl Meteorol 23:201–213
Wilson RJS, Luckman BH (2003) Dendroclimatic reconstruction of maximum summer temperatures from upper tree-line sites in interior British Columbia. Holocene 13:853–863
Wilson RJS, Luckman BH, Esper J (2005) A 500 year dendroclimatic reconstruction of spring-summer precipitation from the lower Bavarian Forest region, Germany. Int J Cliomatol 25:611–630
Xoplaki E, Maheras P, Luterbacher J (2001) Variability of climate in meridional Balkans during the periods 1675–1715 and 1780–1830 and its impact on human life. Clim Change 48:581–615
Xoplaki E, Gonzalez-Rouco FJ, Luterbacher J, Wanner H (2003) Mediterranean summer air temperature variability and its connection to the large-scale atmospheric circulation and SSTs. Clim Dyn 20:723–739
Xoplaki E, Gonzalez-Rouco JF, Luterbacher J, Wanner H (2004) Wet season Mediterranean precipitation variability: influence of large-scale dynamics and trends. Clim Dyn 23:63–78